A Plant miRNA Contributes to Antibacterial Resistance by Repressing Auxin Signaling

Lionel Navarro *et al.*

Science **312**, 436 (2006);
DOI: 10.1126/science.1126088

in the long run. However, migration rate in our experiment was density independent and migration was confined to the two nearest neighbors, whereas it is known that the dynamics of a metapopulation can vary depending on the exact form of density dependence (*31*) and scheme of migration (*11*). Moreover, growth rates of *Drosophila* (and most insects, microbes, and fishes) are higher than those of mammals and birds, which are generally of greater concern for conservation. The intrinsic growth rates of subpopulations are also known to interact strongly with migration rate in producing observed metapopulation dynamics (*12*). Therefore, due caution should be exercised when extrapolating our results to natural populations.

References and Notes

1. I. Hanski, *Metapopulation Ecology* (Oxford Univ. Press, New York, 1999).
2. M. Gyllenberg, G. Söderbacka, S. Ericsson, *Math. Biosci.* **118**, 25 (1993).
3. B. E. Kendall, G. A. Fox, *Theor. Popul. Biol.* **54**, 11 (1998).
4. A. Hastings, *Ecology* **74**, 1362 (1993).
5. J. C. Allen, W. M. Schaffer, D. Rosko, *Nature* **364**, 229 (1993).
6. G. D. Ruxton, *Proc. R. Soc. London Ser. B* **256**, 189 (1994).
7. E. Ranta, V. Kaitala, P. Lundberg, *Oikos* **83**, 376 (1998).
8. J. Ripa, *Oikos* **89**, 175 (2000).
9. G. Nachman, *J. Anim. Ecol.* **56**, 267 (1987).
10. G. Nachman, *Biol. J. Linn. Soc.* **42**, 285 (1991).
11. D. J. D. Earn, S. A. Levin, P. Rohani, *Science* **290**, 1360 (2000).
12. S. Dey, S. Dabholkar, A. Joshi, *J. Theor. Biol.* **238**, 78 (2006).
13. L. D. Mueller, A. Joshi, *Stability in Model Populations* (Princeton Univ. Press, Princeton, NJ, 2000).
14. J. Lecomte, K. Boudjemadi, F. Sarrazin, K. Cally, J. Clobert, *J. Anim. Ecol.* **73**, 179 (2004).
15. R. Levins, *Bull. Entomol. Soc. Am.* **15**, 237 (1969).
16. G. D. Ruxton, *J. Anim. Ecol.* **65**, 161 (1996).
17. I. Hanski, D. Y. Zhang, *J. Theor. Biol.* **163**, 491 (1993).
18. G. Nachman, *Oikos* **91**, 51 (2000).
19. A. R. Ives, S. T. Woody, E. V. Nordheim, C. Nelson, J. H. Andrews, *Am. Nat.* **163**, 375 (2004).
20. In the experiment, the nine subpopulations (single-vial *Drosophila* cultures) were arranged on the periphery of a circle, with each vial exchanging migrants only with its two nearest neighbors (i.e., a one-dimensional array with periodic boundary conditions). In nature, such metapopulations might exist, for example, on the shorelines of lakes or along the edges of ecosystems. The simulations mimicked the experimental system and focused on the behavior of nine coupled Ricker maps, with periodic boundary conditions. See supporting material on *Science* Online.
21. V. Grimm, C. Wissel, *Oecologia* **109**, 323 (1997).
22. We define a population whose size fluctuates with higher amplitude across time to be less stable than one that has lower amplitude of fluctuation ["constancy" attribute of stability (*21*)]. We introduce a measure of stability, the fluctuation index (FI) of a series, given as

$$\mathrm{FI} = \frac{1}{T\overline{N}} \sum_{t=0}^{T-1} \mathrm{abs}(N_{t+1} - N_t)$$

where $\overline{N}$ is the mean population size over T generations. FI thus reflects the mean one-step change in population size, scaled by average population size, over the study duration.
23. O. N. Bjørnstad, R. A. Ims, X. Lambin, *Trends Ecol. Evol.* **14**, 427 (1999).
24. P. A. P. Moran, *Aust. J. Zool.* **1**, 291 (1953).
25. In the experiment, a subpopulation was deemed extinct when it did not contain at least one male and one female fly. When a CM subpopulation became extinct, it was restarted using four males and four females from a backup vial. The backup vials were maintained in parallel to the three treatments, under high larval crowding and yeast supplement to the adults. There were no restarts in LMMs or HMMs; extinct subpopulation vials remained empty until recolonized by migrants from a neighboring subpopulation.
26. Å. Brännström, D. J. T. Sumpter, *Proc. R. Soc. London Ser. B* **272**, 2065 (2005).
27. R. M. May, G. F. Oster, *Am. Nat.* **110**, 573 (1976).
28. For example, in simulations with $r = 2.8$, comparable to the estimated r in our CM subpopulations, the mean extinction rate was 0.75 out of 9 subpopulations per generation, versus 3.35 out of 9 for experimental CMs.
29. R. A. Cheke, J. Holt, *Ecol. Entomol.* **18**, 109 (1993).
30. V. Sheeba, A. Joshi, *Curr. Sci.* **75**, 1406 (1998).
31. R. A. Ims, H. P. Andreassen, *Proc. R. Soc. London Ser. B* **272**, 913 (2005).

32. We thank V. K. Sharma for useful discussions; three anonymous reviewers for helpful comments on the manuscript; M. Shakarad, M. Rajamani, and N. Raghavendra for crucial help in fly handling; and J. Mohan, S. Ghosh, K. M. Satish, N. Rajanna, and M. Manjesh for help in diverse ways during the experiment. Supported by a senior research fellowship from the Council for Scientific and Industrial Research, Government of India (S.D.) and by grants from Department of Science and Technology, Government of India.

Supporting Online Material

www.sciencemag.org/cgi/content/full/312/5772/434/DC1
Materials and Methods
SOM Text
Fig. S1
References

24 January 2006; accepted 16 March 2006
10.1126/science.1125317

A Plant miRNA Contributes to Antibacterial Resistance by Repressing Auxin Signaling

Lionel Navarro,[1,2] Patrice Dunoyer,[2] Florence Jay,[2] Benedict Arnold,[3] Nihal Dharmasiri,[4] Mark Estelle,[4] Olivier Voinnet,[2]*† Jonathan D. G. Jones[1]*†

Plants and animals activate defenses after perceiving pathogen-associated molecular patterns (PAMPs) such as bacterial flagellin. In *Arabidopsis*, perception of flagellin increases resistance to the bacterium *Pseudomonas syringae*, although the molecular mechanisms involved remain elusive. Here, we show that a flagellin-derived peptide induces a plant microRNA (miRNA) that negatively regulates messenger RNAs for the F-box auxin receptors TIR1, AFB2, and AFB3. Repression of auxin signaling restricts *P. syringae* growth, implicating auxin in disease susceptibility and miRNA-mediated suppression of auxin signaling in resistance.

Plants perceive a 22–amino acid peptide (flg22) from the N terminus of eubacterial flagellin (*1*). In *Arabidopsis*, flg22 triggers rapid changes in transcript levels, including down-regulation of a gene subset, potentially by posttranscriptional mechanisms (*2*). One posttranscriptional mechanism is RNA silencing, a sequence-specific mRNA degradation process mediated by 20- to 24-nucleotide (nt) RNAs known as short interfering RNAs (siRNAs) and microRNAs (miRNAs). Both are made from double-stranded RNA (dsRNA) by the ribonuclease III enzyme Dicer. Four paralogs (Dicer-likes, or DCLs) are found in *Arabidopsis*. DCL2 produces viral-derived siRNAs (*3*) and siRNAs from antisense overlapping transcripts (*4*). DCL3 generates DNA repeat–associated siRNAs (*3*), whereas DCL4 synthesizes trans-acting siRNAs and mediates RNA interference (*5*–*7*). DCL1 excises miRNAs from intergenic stem-loop transcripts to promote cleavage of cellular transcripts carrying miRNA-complementary sequences (*8*).

We examined whether small RNAs—especially miRNAs—contribute to the rapid changes elicited by flg22. We analyzed transgenic *Arabidopsis* expressing the P1-Hc-Pro, P19, and P15 viral proteins that suppress miRNA- and siRNA-guided functions (*9*, *10*), anticipating that transcripts repressed by flg22-stimulated small RNAs would be more abundant in these lines. Comparative transcript profiling of untreated

[1]The Sainsbury Laboratory, John Innes Centre, Colney Lane, Norwich NR4 7UH, UK. [2]Institut de Biologie Moléculaire des Plantes du Centre National de la Recherche Scientifique, 67084 Strasbourg Cedex, France. [3]John Innes Centre, Colney Lane, Norwich NR4 7UH, UK. [4]Department of Biology, Indiana University, Bloomington, IN 47405, USA.

*These authors contributed equally to this work.
†To whom correspondence should be addressed. E-mail: jonathan.jones@sainsbury-laboratory.ac.uk (J.D.G.J.); olivier.voinnet@ibmp-ulp.u-strasbg.fr (O.V.)

transgenic seedlings and flg22-elicited wild-type seedlings identified a subset of mRNAs that fulfilled this criterion, including TIR1 (Transport Inhibitor Response 1) and two of its three functional paralogs, AFB2 and AFB3 (Auxin signaling F-Box proteins 2 and 3) (fig. S1, A and B). However, accumulation of AFB1, the third TIR1 paralog, was not discernibly altered in the suppressor lines (fig. S1B).

The F-box proteins TIR1, AFB1, AFB2, and AFB3 are receptors for the plant hormone auxin (*11*–*13*). Additionally, TIR1 and AFB transcripts are targets of miR393, a conserved miRNA (fig. S2) (*14*, *15*). A modified rapid amplification of cDNA ends (RACE) assay confirmed that TIR1, AFB2, and AFB3 mRNAs are specifically cleaved by miR393 in a DCL1-dependent manner (Fig. 1A and fig. S3). However, polymerase chain reaction (PCR)–amplified cleavage products derived from AFB1 were hardly detectable and rarely cloned (Fig. 1A and fig. S3), confirming that AFB1 is partially resistant to miR393-directed cleavage. Presumably, this is due to a single mismatch in the miR393 complementary site found specifically in AFB1 mRNA (fig. S3).

Quantitative reverse transcription–polymerase chain reaction (RT-qPCR) analyses with primers flanking the miR393 target sites revealed a two- to threefold reduction in the levels of TIR1, AFB1, AFB2, and AFB3 30 min after flg22 elicitation of wild-type seedlings (Fig. 1B). Repression of TIR1, AFB2, and AFB3 was partially compromised in *dcl1-9* seedlings (Fig. 1B), suggesting that a miRNA-directed pathway, probably involving miR393, contributes to TIR1, AFB2, and AFB3 down-regulation. However, flg22-triggered down-regulation of AFB1 was unaffected in *dcl1-9*, in agreement with its reduced sensitivity to miR393 (Fig. 1A and fig. S3). Therefore, repression of AFB1 is miRNA-independent and may exclusively occur at the transcriptional level.

We analyzed miR393 levels in flg22-elicited *Arabidopsis* seedlings. Northern analysis showed a twofold increase in miR393 accumulation after 20 and 60 min, whereas levels of the unrelated miR171 remained unaltered (Fig. 2A). Similarly, miR393 levels were unaltered in seedlings treated with control flg22$^{A.tum}$ inactive peptide (Fig. 2A) (*1*). The *Arabidopsis* genome contains two miR393 precursors, on chromosomes 2 (*At-miR393a*) and 3 (*At-miR393b*) (*16*). We fused 1.5-kb DNA fragments upstream of *At-miR393a* and *At-miR393b* to the *enhanced Green Fluorescence Protein* (*eGFP*) and transformed them into *Arabidopsis*, producing transgenic lines *AtmiR393a-p*::*eGFP* and *AtmiR393b-p*::*eGFP*. Using RT-qPCR, we observed a twofold increase in eGFP mRNA level in three independent flg22-treated *AtmiR393a-p*::*eGFP* lines (Fig. 2B), consistent with the miR393 Northern analysis (Fig. 2A). However, eGFP levels were unaltered in three independent *At-miR393b-p*::*eGFP*–elicited lines (Fig. 2B). These data suggest that up-regulation of miR393 by flg22 results from enhanced transcription of *At-miR393a*.

To assay TIR1 protein levels after flg22 treatment, we used *Arabidopsis* transformants expressing a Myc epitope–tagged TIR1 under the dexamethasone (Dex)-inducible promoter (Dex::TIR1-Myc) (*12*). Western blotting revealed a rapid reduction in TIR1-Myc levels upon flg22, but not flg22$^{A.tum}$, treatment (Fig. 3A). Because TIR1 is part of the ubiquitin-ligase complex SCF^{TIR1} that interacts with Aux/IAA proteins to promote their degradation (*17*), we investigated whether Aux/IAA proteins became stabilized upon flg22 treatment. We used transgenic lines expressing a

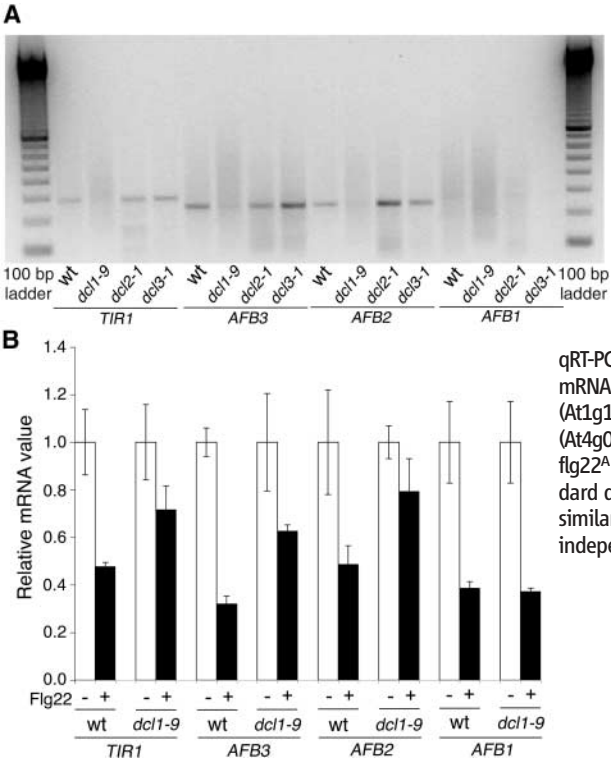

Fig. 1. Flg22 triggers a reduction in TIR1 and AFB mRNAs through miRNA-dependent and miRNA-independent regulatory mechanisms. (**A**) PCR-amplified cleavage products from TIR1 and AFB mRNAs. Col-0 samples are not shown (*27*). (**B**) Repression of TIR1, AFB1, AFB2, and AFB3 mRNAs in response to flg22. Seedlings were treated for 30 min with either 10 μM flg22 (+) or 10 μM flg22$^{A.tum}$ (−). qRT-PCRs were done to assess the relative mRNA levels of TIR1 (At3g62980), AFB3 (At1g12820), AFB2 (At3g26810), and AFB1 (At4g03190) upon treatment with flg22 or flg22$^{A.tum}$. Error bars represent the standard deviation from four PCR results, and similar results were obtained in three independent experiments.

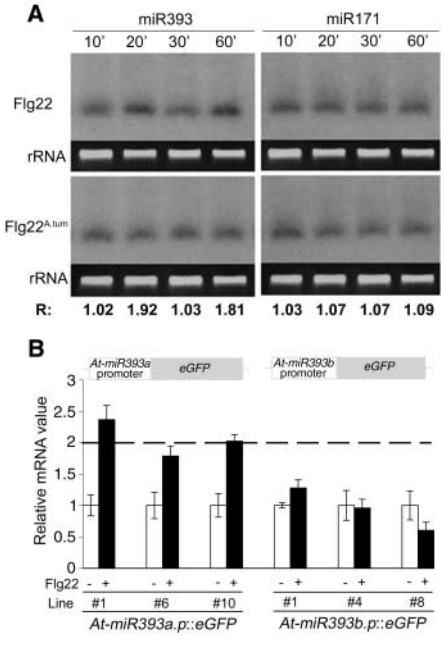

Fig. 2. Flg22 triggers miR393 induction mainly through transcriptional activation of *At-miR393a*. (**A**) Northern analysis of miR393 (left panels) and miR171 (right panels) upon treatment with flg22 (upper panels) or flg22$^{A.tum}$ (bottom panels). Col-0 seedlings were treated with either 10 μM flg22 or 10 μM flg22$^{A.tum}$. rRNA, ethidium bromide staining of ribosomal RNA; R, miRNA signal ratio between flg22-treated versus flg22$^{A.tum}$-treated samples at each time point. (**B**) Transcriptional activation of *At-miR393a* in response to flg22. T2 transgenic lines were treated for 60 min with either 10 μM flg22 (+) or 10 μM flg22$^{A.tum}$ (−). Bar graph representing the relative mRNA level of eGFP upon treatment with flg22 (+) versus flg22$^{A.tum}$ (−) as assayed by qRT-PCR. Error bars represent the standard deviation from three PCR results, and similar results were obtained in two independent experiments. *At-miR393a-p::eGFP* and *At-miR393b-p::eGFP* represent transgenic lines expressing miR393a and miR393b promoter-eGFP fusions, respectively. The dashed line indicates the twofold threshold induction observed in three independent flg22-treated *At-miR393a-p::eGFP* lines.

heat shock–inducible AXR3/IAA17 protein fused to the β-glucuronidase (GUS) reporter (HS::AXR3NT-GUS) (*17*). Seedlings were treated with either flg22 or flg22$^{A.tum}$ for 2 hours at 37°C and then stained for GUS. Flg22, but not flg22$^{A.tum}$, triggered stabilization of AXR3NT-GUS (Fig. 3B), starting from 1.5 hours after flg22 elicitation (Fig. 3C), which coincided with the TIR1-Myc repression (Fig. 3A).

Aux/IAA proteins repress auxin signaling through heterodimerization with Auxin Response Factors (ARFs) (*18*). Those transcription factors ARFs bind to auxin-responsive elements (AuxREs) in promoters of primary auxin-response genes and activate (or repress) transcription (*19*). The flg22-induced stabilization of AXR3/IAA17 prompted us to determine whether flg22 inhibits auxin-response gene activation. Seedlings were treated for 1.5 hours with either flg22 or flg22$^{A.tum}$, and transcripts of the primary auxin-response genes *GH3-like*, *BDL/IAA12*, and *AXR3/IAA17* were monitored by RT-qPCR. This time point was chosen on the basis of the flg22-induced stabilization profile of AXR3/IAA17 (Fig. 3C). All three auxin-response genes were repressed at this time point (Fig. 3D). Thus, flg22 triggers events that contribute to rapid down-regulation of primary auxin-response genes.

Does repression of auxin signaling enhance bacterial disease resistance? We tested, in a *tir1-1* mutant background, resistance in *Arabidopsis* transgenic lines that constitutively overexpress Myc epitope–tagged *AFB1* (*20*). These lines contain higher levels of AFB1 mRNA as compared with *tir1-1*, and exhibit high AFB1-Myc protein accumulation (Fig. 4A). The partial resistance of AFB1 mRNA to miR393, together with its constitutive overexpression, suggested that both AFB1 mRNA and AFB1-Myc would remain unaffected by flg22 treatment, which was confirmed in semiquantitative RT-PCR and Western analysis (Fig. 4, B and C). We anticipated that constitutive overexpression of AFB1 would prevent the miR393-mediated suppression of auxin signaling, perhaps resulting in enhanced disease sensitivity. When AFB1-Myc–overexpressing plants were inoculated with virulent *P. syringae* pv. tomato (Pto) DC3000, they had bacterial titers that were about 20-fold higher than those of nontransformed or *tir1-1* plants and they displayed enhanced disease symptoms (Fig. 4D, fig. S4A). Furthermore, no difference was observed with avirulent Pto DC3000 carrying *AvrRpt2*, which triggers race-specific resistance via resistance gene *RPS2* (Fig. 4E) (*21*). Thus, suppression of auxin signaling, mediated at least partly by miR393, might specifically promote resistance to virulent Pto DC3000 but is not implicated in race-specific resistance.

We also transformed *Arabidopsis* with a construct with *At-miR393a* constitutively transcribed from the strong 35*S* promoter (Fig. 4F). Three independent T2 transgenic lines were selected for high miR393 accumulation (Fig. 4F). These lines showed lower TIR1 mRNA levels than controls (Fig. 4F), and in older plants, they displayed reduced apical dominance with multiple shoots, reminiscent of auxin signaling mutants. However, these developmental alterations were minor compared with those observed in *tir1/afb* multiple mutants (*20*). Four days after inoculation with virulent Pto DC3000, all three miR393-overexpressing lines, but not the controls, displayed fivefold lower bacterial titer, confirming that miR393 restricts Pto DC3000 growth (Fig. 4G). There was no difference in bacterial growth on transgenic lines overexpressing an artificial miRNA directed against GFP (*22*) (Fig. 4G).

We show here that a bacterial PAMP down-regulates auxin signaling in *Arabidopsis* by targeting auxin receptor transcripts. Augmenting auxin signaling through overexpressing a *TIR1* paralog that is partially refractory to miR393 enhances susceptibility to virulent Pto DC3000, and, conversely, repressing auxin signaling through miR393 overexpression increases bacterial resistance. These results indicate that down-regulation of auxin signaling, resulting in ARF inactivation, is part of a plant-induced immune response (fig. S5). They also suggest that auxin promotes susceptibility to bacterial disease. This is consistent with other published findings. The tumorigenic *P. syringae* pv. *savastonoi* synthesizes high levels of indole-3-acetic acid (IAA) (*23*). Also, most *P. syringae* strains can produce IAA, and Pto DC3000 infection triggers increased IAA levels in *Arabidopsis* (*24*, *25*). Consistent with these observations, exogenous application of the auxin analog 2,4-dichlorophenoxyacetic acid enhances Pto DC3000 disease symptoms (fig. S4B).

In addition to the contribution of miR393 in flg22-triggered repression of auxin signaling, our analysis also reveals a miR393-

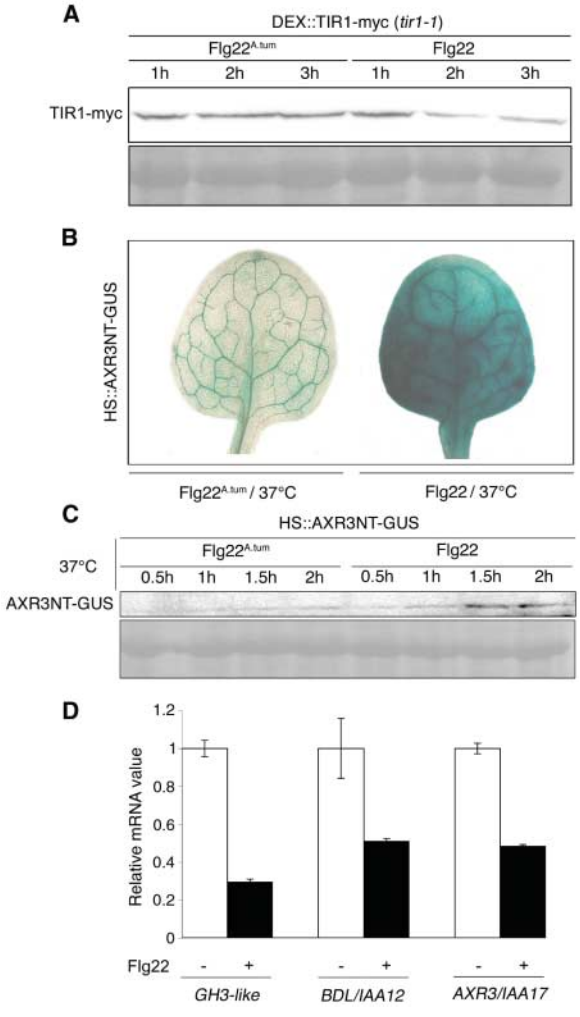

Fig. 3. Flg22 triggers repression of TIR1 protein, stabilization of AXR3/IAA17, and repression of three primary auxin-response transcripts. (**A**) TIR1-Myc repression in response to flg22. (Upper panel) Western analysis using a Myc-specific antibody (anti-Myc). (Bottom panel) Ponceau staining of total proteins. Similar results were obtained in two independent experiments. (**B**) AXR3/IAA17 stabilization in leaves. HS::AXR3NT-GUS seedlings were transferred for 2 hours at 37°C with either 10 μM flg22 (right leaf) or 10 μM flg22$^{A.tum}$ (left leaf). Similar results were obtained in five independent experiments. (**C**) Kinetics of AXR3/IAA17 stabilization. HS::AXR3NT-GUS seedlings were treated as in (B). (Upper panel) Western analysis using anti-GUS. (Bottom panel) Ponceau staining of total proteins. Similar results were obtained in two independent experiments. (**D**) Flg22 reduces accumulation of three primary auxin-response genes. Col-0 seedlings were treated for 1.5 hours with either 10 μM flg22 (+) or 10 μM flg22$^{A.tum}$ (−). qRT-PCRs were done to assess the relative mRNA level of GH3-like (At4g03400), BDL/IAA12 (At1g04550), and AXR3/IAA17 (At1g04250) upon flg22 as compared with flg22$^{A.tum}$ treatment. Error bars represent the standard deviation from four PCR results, and similar results were obtained in three independent experiments.

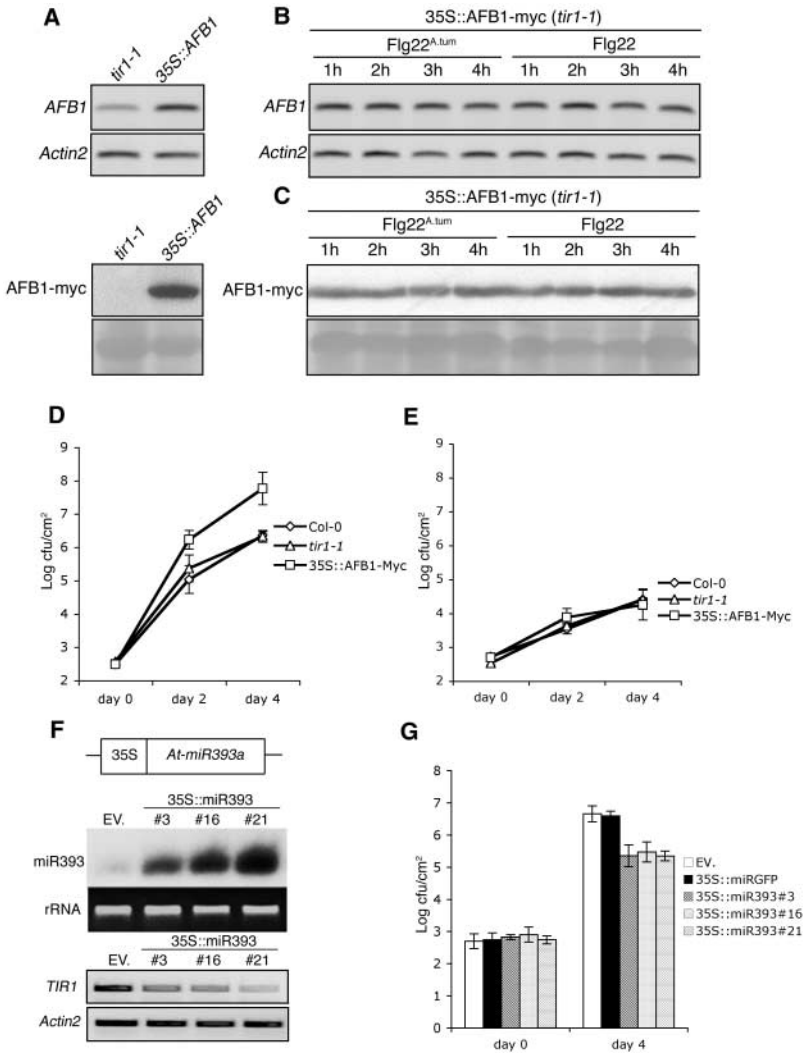

Fig. 4. Down-regulation of auxin signaling is required for Pto DC3000 disease resistance. (**A**) Molecular characterization of AFB1-overexpressing lines. (Upper panel) RT-PCR analysis of AFB1 transcript. (Bottom panel) Western analysis using anti-Myc. (**B**) AFB1 mRNA levels are not altered in AFB1-overexpressing lines treated with flg22. The 35S::AFB1-Myc seedlings were treated with either 10 μM flg22 or 10 μM flg22$^{A.tum}$. RT-PCR analysis was done as in (A). (**C**) AFB1-Myc protein levels are not altered in AFB1-overexpressing challenged lines. The 35S::AFB1-Myc seedlings were treated as in (B). (Upper panel) Western analysis using anti-Myc. (Bottom panel) Ponceau staining of total proteins. (**D**) Growth of Pto DC3000 on AFB1-overexpressing lines. Six-week-old plants were inoculated with 10^5 colony-forming units (cfu/ml) of bacteria. Error bars represent the standard error of log-transformed data from five independent samples, and similar results were obtained in three independent experiments. (**E**) Growth of Pto DC3000 (AvrRpt2) on AFB1-overexpressing lines. Inoculation was performed as in (D), and results are presented as in (D). Similar results were obtained in two independent experiments. (**F**) Molecular characterization of miR393-overexpressing lines. (Top panel) Schematic representation of the 35S::*At-miR393a* construct. (**G**) Growth of Pto DC3000 on miR393-overexpressing lines. Inoculation was performed as in (D). Similar results were obtained in two independent experiments. (Middle panel) Northern analysis of miR393 overexpression in independent T2 transgenic lines; EV, empty vector; rRNA, ethidium bromide staining of ribosomal RNA. (Bottom panel) RT-PCR of the TIR1 transcript.

independent pathway that probably involves transcriptional repression of *TIR1* and its paralogs. This is consistent with "mutual exclusion" in *Drosophila*, whereby miRNAs prevent unwanted expression of genes that become transcriptionally repressed in the miRNA-producing cells (*26*). Rapid induction of miR393 by flg22 might deplete TIR1 mRNAs present at the time of elicitation and thus confer robustness to the transcriptional repression provoked during elicitation. This regulatory feature has not previously been reported for plant miRNAs involved in development, and it will be interesting to establish if these observations on miR393 hold for other stress-induced miRNAs.

References and Notes

1. G. Felix, J. D. Duran, S. Volko, T. Boller, *Plant J.* **18**, 265 (1999).
2. L. Navarro *et al.*, *Plant Physiol.* **135**, 1113 (2004).
3. Z. Xie *et al.*, *PLoS Biol.* **2**, E104 (2004).
4. O. Borsani, J. Zhu, P. E. Verslues, R. Sunkar, J. K. Zhu, *Cell* **123**, 1279 (2005).
5. Z. Xie, E. Allen, A. Wilken, J. C. Carrington, *Proc. Natl. Acad. Sci. U.S.A.* **102**, 12984 (2005).
6. V. Gasciolli, A. C. Mallory, D. P. Bartel, H. Vaucheret, *Curr. Biol.* **15**, 1494 (2005).
7. P. Dunoyer, C. Himber, O. Voinnet, *Nat. Genet.* **37**, 1356 (2005).
8. D. P. Bartel, *Cell* **116**, 281 (2004).
9. P. Dunoyer, C. H. Lecellier, E. A. Parizotto, C. Himber, O. Voinnet, *Plant Cell* **16**, 1235 (2004).
10. E. J. Chapman, A. I. Prokhnevsky, K. Gopinath, V. V. Dolja, J. C. Carrington, *Genes Dev.* **18**, 1179 (2004).
11. N. Dharmasiri, S. Dharmasiri, M. Estelle, *Nature* **435**, 441 (2005).
12. W. M. Gray *et al.*, *Genes Dev.* **13**, 1678 (1999).
13. S. Kepinski, O. Leyser, *Nature* **435**, 446 (2005).
14. M. W. Jones-Rhoades, D. P. Bartel, *Mol. Cell* **14**, 787 (2004).
15. R. Sunkar, J. K. Zhu, *Plant Cell* **16**, 2001 (2004).
16. A. M. Gustafson *et al.*, *Nucleic Acids Res.* **33**, D637 (2005).
17. W. M. Gray, S. Kepinski, D. Rouse, O. Leyser, M. Estelle, *Nature* **414**, 271 (2001).
18. E. Liscum, J. W. Reed, *Plant Mol. Biol.* **49**, 387 (2002).
19. G. Hagen, T. Guilfoyle, *Plant Mol. Biol.* **49**, 373 (2002).
20. N. Dharmasiri *et al.*, *Dev. Cell* **9**, 109 (2005).
21. M. C. Whalen, R. W. Innes, A. F. Bent, B. J. Staskawicz, *Plant Cell* **3**, 49 (1991).
22. E. A. Parizotto, P. Dunoyer, N. Rahm, C. Himber, O. Voinnet, *Genes Dev.* **18**, 2237 (2004).
23. T. Yamada *et al.*, in *Molecular Strategies of Pathogens and Host Plants*, D. L. Mills, C. Vance, S. Ouchi, S. S. Patil, Eds. (Springer, New York, 1991), pp. 83–94.
24. E. Glickmann *et al.*, *Mol. Plant Microbe Interact.* **11**, 156 (1998).
25. P. J. O'Donnell *et al.*, *Plant J.* **33**, 245 (2003).
26. A. Stark, J. Brennecke, N. Bushati, R. B. Russell, S. M. Cohen, *Cell* **123**, 1133 (2005).
27. Materials and methods are available as supporting material on *Science* Online.

28. We thank B. Kunkel and P. Brodersen for helpful comments and L. Buhot for technical advice. Supported by the Gatsby Foundation (J.D.G.J); a long-term Fellowship from the Federation of European Biochemical Societies and by the Gatsby Foundation (L.N.); an Action Thématique Incitative sur Programme grant from the CNRS and a grant from the trilateral génoplante–German Plant Genome Research Program–Spanish ministry of Research (P.D, F.J, and O.V); and by grants from NIH, NSF, and the U.S. Department of Energy (N.D and M.E.)

Supporting Online Material

www.sciencemag.org/cgi/content/full/312/5772/436/DC1
Materials and Methods
SOM Text
Figs. S1 to S5
References

10 February 2006; accepted 23 March 2006
10.1126/science.1126088